

Ideal 3D asymmetric concentrator

Angel Garcia-Botella^{a,*}, Antonio Alvarez Fernandez-Balbuena^{b,1}, Daniel Vázquez^{b,1},
Eusebio Bernabeu^{b,1}

^a *Departamento Física Aplicada a los Recursos Naturales, Universidad Politécnica de Madrid, E.T.S.I. de Montes, Ciudad Universitaria s/n, 28040 Madrid, Spain*

^b *Departamento de Óptica, Universidad Complutense de Madrid, Fac. CC. Físicas, Ciudad Universitaria s/n, 28040 Madrid, Spain*

Received 10 July 2007; received in revised form 23 April 2008; accepted 14 July 2008

Available online 3 August 2008

Communicated by: Associate Editor Darren Bagnall

Abstract

Nonimaging optics is a field devoted to the design of optical components for applications such as solar concentration or illumination. In this field, many different techniques have been used for producing reflective and refractive optical devices, including reverse engineering techniques. In this paper we apply photometric field theory and elliptic ray bundles method to study 3D asymmetric – without rotational or translational symmetry – concentrators, which can be useful components for nontracking solar applications. We study the one-sheet hyperbolic concentrator and we demonstrate its behaviour as ideal 3D asymmetric concentrator.

© 2008 Elsevier Ltd. All rights reserved.

Keywords: Solar concentration; Concentrators; Optical engineering

1. Introduction

The flow line method is one of the most powerful techniques for designing nonimaging optical devices. Winston and Welford introduced the concept of the geometrical vector flux \mathbf{J} (Winston and Welford, 1979), where the direction of \mathbf{J} is the flow line, and showed that ideal flux concentrators have shapes that do not disturb the geometrical vector flux field. In particular, the compound parabolic concentrator (CPC) is shown as arising from the \mathbf{J} field of a Lambertian emitter in the form of a 2D truncated wedge, and the hyperbolic trumpet is introduced as arising from the \mathbf{J} field of a Lambertian emitter in the form of a disk (Winston et al., 2005). This method is the basis of a more general method for concentrator design, elliptic ray bundles method (Gutiérrez et al., 1996; Benítez, 1999). On

the other side, Moon and Spencer (1981) used a similar concept, the pharosage vector, to study the flux field from Lambertian illuminators, developing the so-called Photoc Field theory, which has been useful for applications like image rendering. Both concepts are completely analogous; the geometrical vector flux \mathbf{J} is mainly focused on the design of nonimaging optics components and the pharosage vector, is focused on the obtaining of photometric data, but both are based on the study of the flow field generated by Lambertian illuminators.

In this paper, we apply principles and results of these theories, to elliptical concentrators (García-Botella et al., 2006), to identify and study ideal 3D asymmetric concentrators which could be of interest in nontracking solar concentration, where 2D asymmetric concentrators have been applied (Mallick et al., 2004). These concentrators will have the shape which does not disturb the geometrical flux vector field generated by an elliptical disk.

This work is organized as follows: in Section 2 we present the theoretical background, focused on the study of the

* Corresponding author. Tel./fax: +34 91 336 7079.

E-mail address: angel.garciab@upm.es (A. García-Botella).

¹ Tel.: +34 91 394 45 55; fax: +34 91 394 46 74.

flux field generated by an elliptical disk and the shape of the ideal elliptical concentrator, in Section 3 we show geometrically the ray propagation inside the ideal elliptical concentrator. In Section 4 we study, by means of Monte-carlo raytracing simulations, the efficiency of this concentrator, showing its ideal behaviour. Finally, in Section 5, conclusions are presented.

2. Theoretical background

The flow line method was introduced by Winston and Welford (1979), based on the concept of the geometrical vector flux \mathbf{J} , from the application of the etendue conservation law for a loss-free optical system. The components of the geometrical vector flux are

$$J_z = \int dp_x dp_y, \quad J_x = \int dp_y dp_z, \quad J_y = \int dp_x dp_z, \quad (1)$$

where p_x, p_y and p_z are the optical direction cosines, or, for more general considerations, the generalized momenta in phase space. The physical meaning of the geometrical vector flux is as follows: the J_z component, for instance, is proportional to the total flux per unit area entering the plane x, y at point $P(x, y, z)$, and similarly for the other vector components. The flow line is the direction of \mathbf{J} vector, and its most important property is that a way to construct a concentrator with maximum theoretical concentration ratio is to place mirrors in the flow lines under conditions of detailed balance of rays, which means that for each ray r_1 incident on one side of this mirror surface, there must be a corresponding ray r_2 incident on the other side such as that r_2 is in the direction of the reflection of r_1 .

In an analogous way, Moon and Spencer (1981), introduced the concept of pharosage vector \mathbf{D} (*Pharos* is the Greek word for “lighthouse” and the *age* suffix indicates “per unit area”) associated with any point $P(x, y, z)$ of the space. The magnitude of the pharosage vector is equal to the net radiant power per unit area at P , and the direction of the vector is the direction of the flow of the radiant energy at that point. Then, the unique difference between geometrical flux vector and pharosage vector is a constant k ,

$$\mathbf{D} = k\mathbf{J}. \quad (2)$$

For our purposes, we will use the results of Photic field theory to study the flow lines generated by an elliptical disk. In this sense we can use the vector potential employed by Moon and Spencer (1981), a concept which was introduced by Fock (1924), from the application of the Stokes theorem to the evaluation of irradiance integral over a light source of uniform radiance, at any point P (Fig. 1),

$$k\mathbf{J} = \int_s \frac{L \cos \theta}{r^2} \mathbf{r}_1 ds = \int_s \frac{L \mathbf{r}_1}{r^2} (\mathbf{r}_1 \cdot \mathbf{n}_1) ds, \quad (3)$$

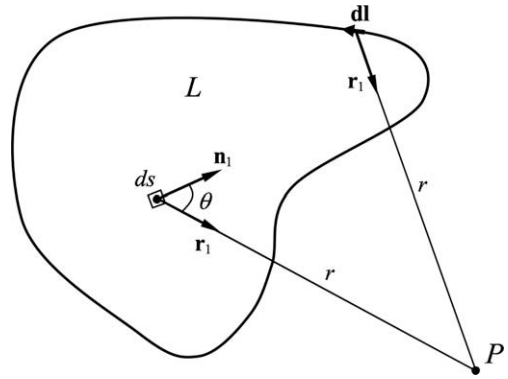


Fig. 1. Contour integration and parameters for surface source of uniform radiance.

where L is the radiance of the source, \mathbf{r}_1 is the unit vector in the direction of r , \mathbf{n}_1 is the surface normal vector and θ the angle between \mathbf{r}_1 and \mathbf{n}_1 . If L is constant, as it is for the Lambertian surface, by using the Stokes theorem we have (Moon and Spencer, 1981),

$$k\mathbf{J} = \frac{L}{2} \oint \mathbf{dl} \times \frac{\mathbf{r}_1}{r}, \quad (4)$$

but

$$\frac{\mathbf{r}_1}{r} = \text{grad}(\ln r), \quad (5)$$

and, taking into account that,

$$\text{grad } u \times \mathbf{v} = \text{curl}(u\mathbf{v}) - u\text{curl}\mathbf{v}, \quad (6)$$

Eq. (4) becomes

$$k\mathbf{J} = -\frac{L}{2} \oint \text{curl}(\ln r \mathbf{dl}) = \text{curl}\left(-\frac{L}{2} \oint \ln r \mathbf{dl}\right), \quad (7)$$

then $k\mathbf{J} = \text{curl } \mathbf{A}$, and we can introduce the Fock’s expression for the vector potential

$$\mathbf{A} = -\frac{L}{2} \oint \ln r \mathbf{dl}. \quad (8)$$

From this result, Fock (Fock, 1924) studied as examples the distribution of \mathbf{J} vector from an elliptical disk with $L = \text{const.}$, and showed that the \mathbf{J} vector is always orthogonal to the ellipsoids of equations

$$\frac{x^2}{\lambda} + \frac{y^2}{\lambda - c^2} + \frac{z^2}{\lambda - a^2} = 1, \quad \text{with } \infty > \lambda > a^2 \quad (9)$$

where λ is the parameter for confocal ellipsoids surfaces, $c^2 = a^2 - b^2$ and, a and b are major and minor semiaxes of the elliptic disk. Then the surfaces which can follow the direction of \mathbf{J} vector, orthogonal to the ellipsoids, are one-sheeted hyperboloids of equations

$$\frac{x^2}{\mu} + \frac{y^2}{\mu - c^2} + \frac{z^2}{\mu - a^2} = 1, \quad \text{with } a^2 > \mu > c^2, \quad (10)$$

and, then, using the main property of the \mathbf{J} vector, and taking into account that we have used a lambertian elliptical disk as source, which fulfils the condition of detailed balance of rays, we can say that concentrators with one-

sheet hyperbolic geometry can be considered as concentrators with maximum theoretical concentration ratio. From the definition and classification of concentrators (Winston et al., 2005), (Garcia-Botella et al., 2006), one-sheet hyperbolic concentrator is an ideal finite source non-homofocal elliptical concentrator.

On the other hand, it is possible to arrive to the same result applying the elliptic ray bundle method (Gutiérrez et al., 1996), when the parameters of the bundle take the values,

$$a = 1, \quad b_1 = b_2 = b_3 = d = k = l = n = 0, \quad m = a^2, \quad p = b^2, \quad (11)$$

in the \mathbf{G}^{-1} matrix, which provides solutions for the vector flux field.

3. Ray propagation in one-sheet hyperbolic concentrator

Once we have introduced the theoretical background based on the study of flow lines, we shall study the behaviour of rays inside one-sheet hyperbolic reflector. To start, we can use the standard equation for a one-sheet hyperboloid

$$\frac{x^2}{a^2} + \frac{y^2}{b^2} - \frac{z^2}{c^2} = 1, \quad (12)$$

where a , b and c are the geometrical parameters of the concentrator.

From the definition of one-sheet hyperboloid, the meridional sections are hyperbolas with different focal lengths, the foci of this hyperbolas are located on the ellipse of semiaxes $\sqrt{a^2 + c^2}$ and $\sqrt{b^2 + c^2}$. This ellipse forms what we have called a virtual elliptic receiver at the exit aperture. Using the basic property of the 2D hyperbolic reflector (O’Gallagher et al., 1987), any meridional ray aimed to the virtual elliptic receiver at the exit aperture is reflected, by the one-sheet hyperboloid, to some point of this receiver, propagating the ray until it reaches the exit aperture. Nevertheless, to show the ideal behaviour of the one-sheet hyperbolic concentrator, it is necessary to prove that all rays, not only meridional, directed to the virtual elliptic receiver at the exit aperture are reflected by the concentrator to some point on this receiver. To do that, we can use a similar, but more general, proof than used for skew rays in hyperbolic concentrator (Winston et al., 2005). Three properties of one-sheet hyperbolic concentrator geometry are useful: (1) All meridional sections of a one-sheet hyperbolic concentrator are hyperbolas, (2) all cross sections of a one-sheet hyperbolic concentrator are ellipses and (3) the tangent plane, at any point P of a one-sheet hyperbolic concentrator, is defined by the bisector of the angle FPF' , where F and F' are the foci of the hyperbola in the meridional plane (Fig. 2), and the tangent line to the elliptic cross section at P . All the skew rays incident at point P directed to the virtual elliptic receiver generate an oblique elliptical cone, or incident cone. Then, the reflected cone will be the

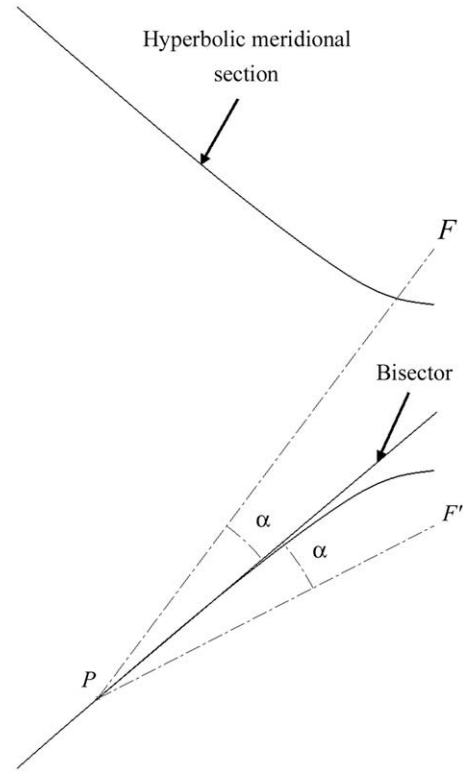


Fig. 2. Bisector of the angle FPF' , at meridional hyperbolic section of one-sheet hyperbolic concentrator.

mirror image of the incident cone, through the tangent plane at point P . By the geometry of this particular problem, the cross section of the incident cone, normal to the bisector of the angle FPF' , is an ellipse (Fig. 3). One of the principal axes of this ellipse lies in the tangent plane of the one-sheet hyperboloid and, by definition, the bisector of the incident cone too; therefore, the tangent plane coincides with a symmetry plane of the incident cone. This produces that the reflected cone coincides with the incident

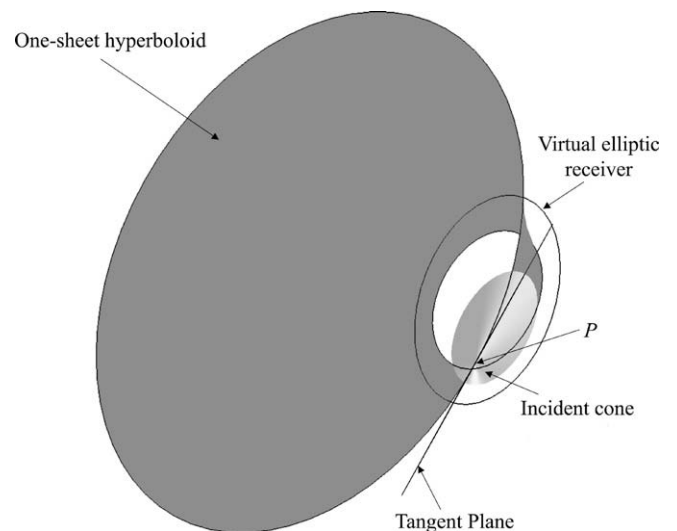


Fig. 3. Front view of incident cone, the tangent plane is the symmetry plane of the cone.

cone (Fig. 4), which means that all rays incident at point P aimed to the virtual elliptic receiver, are reflected by the concentrator to some point on this receiver. This proves that a one-sheet hyperbolic concentrator is an ideal 3D asymmetric concentrator.

4. Simulations in one-sheet hyperbolic concentrator

To show the behaviour of the one-sheet hyperbolic concentrator we have studied its efficiency by raytracing simulations. Because one-sheet hyperbolic concentrators are finite source concentrators, it is necessary to quantify the number of rays linking the input and output surface by the concentrator, and compare it to the number of rays linking the input surface and the virtual elliptic receiver at each incident angle, so we need two raytraces by each measure (angle). To perform these simulations we have employed a perfect one-sheet hyperboloid mirror, reflectance $\rho = 1$, of parameters $a = 50$ mm, $b = 25$ mm, $c = 30$ mm and height $h = 70$ mm (Fig. 5). We have traced a beam of collimated rays, which fills the entry aperture of the concentrator, for different incident angles. For this beam we have measured, on the one hand, the number of rays incident to the virtual elliptic receiver – without the concentrator, and on the other hand, the number of rays emerging from the exit aperture of the one-sheet hyperbolic concentrator after reflection. Fig. 6 shows the ratio between these measurements for all incident angles and for different azimuth angles of incidence. Using the parameters of the employed concentrator, the cutoff angle at minor semiaxis is $\theta_{\max} = 55.7^\circ$ and at major semiaxis is $\theta_{\max} = 69.3^\circ$. Fig. 6 plots the ideal 3D rectangular cutoff behaviour of the one-sheet hyperbolic concentrator, for four azimuth angles of incidence being 0° the direction of minor semiaxis, showing its ideal 3D asymmetrical behaviour, obviously for real reflectance values, around 0.95, the transmission angle curve will reduce its efficiency. It shows too the small simulations errors, which appear near the cut-off angle due to the faceted design of the concentrator.

As we have mentioned, one-sheet hyperbolic concentrator is a finite source ideal concentrator. For nontracking solar concentration applications, infinite source concentrators are needed; then, to obtain a infinite source concentra-

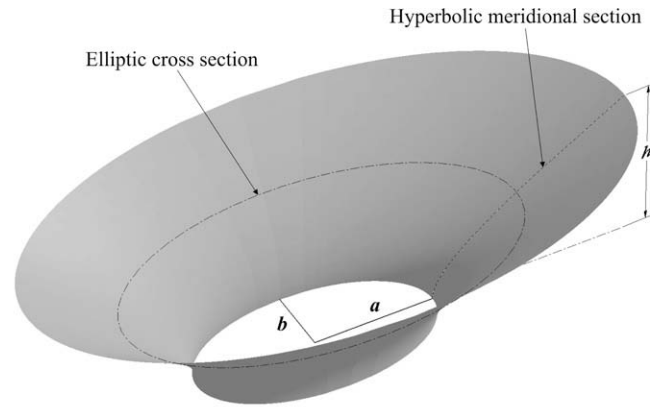


Fig. 5. One-sheet hyperbolic concentrator with parameters $a = 50$ mm, $b = 25$ mm, $c = 30$ mm and $h = 70$ mm.

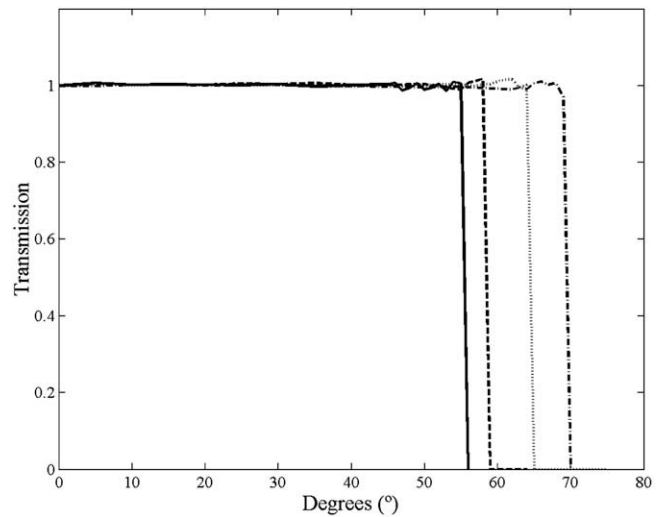


Fig. 6. Transmission-angle curves for one-sheet hyperbolic concentrator, reflectance 1, at several azimuth incidence angles, (—) 0° incidence – minor semiaxes, (---) 30° incidence, (···) 60° incidence and (-·-) 90° incidence – major semiaxes.

tor an asymmetric lens must be added at the entry aperture of the one-sheet hyperbolic concentrator, in a similar way that by O’Gallagher et al. (1987).

5. Conclusions

In this paper, we have applied the results of two analogous photometric theories, elliptic ray bundles method and photic field theory, to study new asymmetric concentrators. By this, we have found that the one-sheet hyperbolic concentrator is an ideal 3D asymmetric concentrator, as its shape does not disturb the flow lines of an elliptical disk. This device can be applied for nontracking solar concentration, where two different acceptance angles, at transversal and longitudinal directions, are needed. Using ray propagation, we have shown that all rays incident on the concentrator, aimed to the virtual elliptic receiver, are reflected to

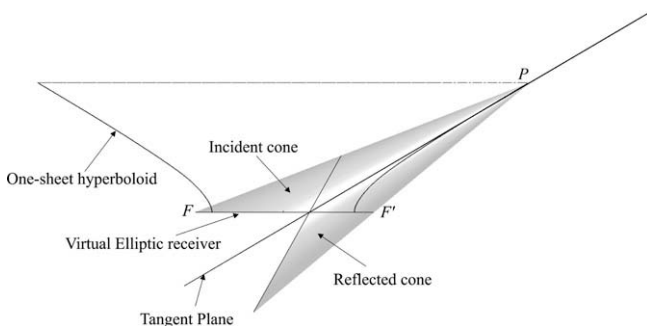


Fig. 4. Incident cone, reflected cone and tangent plane at one-sheet hyperbolic concentrator.

some point on this virtual elliptic receiver, which proves the ideal behaviour of the one-sheet hyperbolic concentrator. Finally, we have studied this concentrator by raytracing simulations, showing the ideal 3D behaviour in transmission angle curves, with different rectangular cutoff transmission angle curves for different azimuth angles of incidence.

Acknowledgements

This research was partially supported by the Comunidad de Madrid project ARCHISENS-CM Programme Ref: S-505/ENE0355. The authors thank to A. Gonzalez-Cano for his suggestions to this work.

References

- Benítez, P., 1999. Elliptic ray bundles in three-dimensional geometry for nonimaging optics: a new approach. *J. Opt. Soc. Am. A* 16 (9), 2245–2252.
- Fock, V., 1924. Zur Berechnung der Beleuchtungsstärke. *Z. Phys.* 28, 102–118.
- Garcia-Botella, A., Fernandez-Balbuena, A.A., Bernabeu, E., 2006. Elliptical concentrators. *Appl. Opt.* 45 (29), 7622–7627.
- Gutiérrez, M., Miñano, J.C., Vega, C., Benítez, P., 1996. Application of Lorentz geometry to nonimaging optics: new three-dimensional ideal concentrators. *J. Opt. Soc. Am. A* 13 (3), 532–540.
- Mallick, T.K., Eames, P.C., Hyde, T.J., Norton, B., 2004. The design and experimental characterisation of an asymmetric compound parabolic photovoltaic concentrator for building façade integration in the UK. *Sol. Energy* 77, 319–327.
- Moon, P., Spencer, D.E., 1981. *Photic Field*. Massachusetts Institute of Technology Press, Massachusetts.
- O’Gallagher, J., Winston, R., Welford, W.T., 1987. Axially symmetric nonimaging flux concentrators with the maximum theoretical concentration ratio. *J. Opt. Soc. Am. A* 4 (1), 66–68.
- Winston, R., Welford, W.T., 1979. Geometrical vector flux and some new nonimaging concentrators. *J. Opt. Soc. Am.* 69 (4), 532–536.
- Winston, R., Miñano, J.C., Benítez, P., with contributions by Shatz, N., Bortz, J.C., 2005. *Nonimaging Optics*. Elsevier Academic Press, New York.